ELSEVIER

Journal of Molecular Catalysis A: Chemical 162 (2000) 431–441

JOURNAL OF MOLECULAR CATALYSIS A: CHEMICAL

www.elsevier.com/locate/molcata

Characterization of $MoO_3/TiO_2–ZrO_2$ catalysts by XPS and other techniques

Benjaram M. Reddy [a,*], B. Chowdhury [a], E.P. Reddy [a,b], A. Fernández [b]

[a] *Inorganic Chemistry Division, Indian Institute of Chemical Technology, Hyderabad 500 007, India*

[b] *Instituto de Ciencia de Materiales de Sevilla, Centro de Investigaciones Científicas Isla de la Cartuja, Avda. Américo Vespucio s / n, 41092 Sevilla, Spain*

Abstract

To explore thermal stability of $TiO_2–ZrO_2$ support, and dispersion and temperature stability of $MoO_3/TiO_2–ZrO_2$ catalyst these systems were subjected to thermal treatments from 773 to 1073 K and were examined by X-ray photoelectron spectroscopy, X-ray diffraction, and FT-infrared techniques. The $TiO_2–ZrO_2$ mixed oxide support was obtained by a homogeneous coprecipitation method and MoO_3 (12 wt.%) was impregnated over the 773 K calcined support by adopting a wet impregnation procedure. Characterization results suggest that the $TiO_2–ZrO_2$ when calcined at 773 K is in X-ray amorphous state and gets converted into a crystalline $ZrTiO_4$ compound beyond 873 K. The $ZrTiO_4$ compound is thermally quite stable up to 1073 K calcination temperature in the absence of molybdena on its surface. In the case of $MoO_3/TiO_2–ZrO_2$ catalyst, the molybdenum oxide is in highly dispersed state on the support surface when calcined at 773 K. However, above 773 K calcination it selectively interacts with ZrO_2 portion of the $TiO_2–ZrO_2$ binary oxide and readily forms $ZrMo_2O_8$ compound by liberating TiO_2. The $ZrMo_2O_8$ compound formation proceeds in a two-step process. In the first step, there is an incorporation of Mo^{6+} ions into the ZrO_2 oxide matrix and then the crystal growth occurs. The liberated TiO_2 appears in the form of both anatase and rutile phases with varying intensities.

Keywords: Molybdena; $TiO_2–ZrO_2$; Mixed oxide; XPS; XRD; Dispersion

1. Introduction

During the last decade, a great deal of fundamental and applied research interest was focused on supported molybdena catalysts because of their numerous applications in petroleum refining, chemicals production and pollution control industries [1,2]. The industrial importance of these catalysts has prompted a large number of characterization studies concerning the surface structure of these catalysts by Fourier transform infrared (FTIR), electron spin resonance (ESR), UV–VIS diffuse reflectance, extended X-ray absorption fine structure (EXAFS), X-ray absorption near edge structure (XANES), solid state ^{95}Mo nuclear magnetic resonance (NMR), Raman spectroscopy, and other methods [3–8]. It has been observed from various investigations that the surface structure of molybdena species is related to the nature, in particular the surface structure, of the support; the extent of surface hydration; the loading amount; and the calcination temperature [1,2,9–14].

The structure of molybdenum oxide on γ-Al_2O_3 has been extensively studied under ambient conditions [11–14]. Besides alumina, considerable interest

* Corresponding author. Fax: +91-40-7170921.
E-mail address: bmreddy@iict.ap.nic.in (B.M. Reddy).

1381-1169/00/$ - see front matter
PII: S1381-1169(00)00336-8

has now been devoted to other supports such as TiO_2, CeO_2, and ZrO_2 in exploring better catalysts through adjusting the interaction strength between the dispersed species and the support. Molybdena–titania combination is an excellent catalyst for selective oxidation of hydrocarbons [15] and selective catalytic reduction (SCR) of NO_x by ammonia [16]. Moreover, they are the precursors of alkene metathesis catalysts [17], and of sulfided hydrodesulfurization catalysts [18]. Eon et al. [19] suggested that molybdena–titania interaction takes place through a perfect adjustment of (0 1 0) planes of MoO_3 with (0 0 1) planes of TiO_2, thus leading to an epitaxial growth in the (0 k 0) direction of MoO_3 crystals over the TiO_2. It is known that crystallographic lattice fitting between the active component and the support lowers the surface energy barriers. Therefore, transfer of electron becomes easy across the solid–solid interface for the supported catalyst.

Zirconia is yet another interesting material and it been increasingly used in catalysis both as a support and as a catalyst [20]. It has been found that Mo/ZrO_2 catalyst exhibits better catalytic properties that Mo/Al_2O_3 for hydrodesulfurization of thiophene [21], hydrogenation of CO [22], and partial oxidation of methanol [23] and ethanol [24]. A specially prepared $Mo–ZrO_2$ also exhibits very string acidic properties, hence find numerous applications in the synthesis of fine chemicals [25]. The intrinsic benign characteristics of both zirconia and titania supports can be explored fully by using them in combination. Thus, the combined $TiO_2–ZrO_2$ mixed oxide has attracted much attention recently as a catalyst and as a support for the various applications. The $TiO_2–ZrO_2$ binary oxide has been reported to exhibit a high surface acidity by a charge imbalance based on the generation of Ti–O–Zr bonding [26]. It is also possible that Ti and Zr ions on the $TiO_2–ZrO_2$ binary oxide may act as acidic and basic sites, respectively, which may serve as catalytic active sites [27]. Recent studies reveal that the $TiO_2–ZrO_2$ is an active catalyst for dehydrocyclization of *n*-paraffins to aromatics [28], hydrogenation of carboxylic acids to alcohols [29], and as a support for MoO_3 based catalysts for hydroprocessing applications [30].

Ng and Gulari [31] have observed a high dispersion of octahedral polymolybdate over titania surface by using laser Raman and IR spectroscopy techniques. Caceres et al. [32] also supported those observations from ESR and XPS measurements. Although two dimensional polymolybdate structures over TiO_2 surface have been suggested from various studies, no information is available about the degree and the way of agglomeration of the basic octahedral units occur to form the surface structure of the dispersed moieties. The aim of the present study is to explore the influence of support on the dispersion behavior of molybdena and the effect of calcination temperature on the final state of the supported oxide species. In this investigation, a $TiO_2–ZrO_2$ binary oxide support was prepared by a homogeneous coprecipitation method and was impregnated with 12 wt.% MoO_3. The $TiO_2–ZrO_2$ support and the $MoO_3/TiO_2–ZrO_2$ catalyst were subjected to thermal treatments from 773 to 1073 K and were examined by XRD, FTIR, and XPS techniques.

2. Experimental

2.1. Catalyst preparation

The $TiO_2–ZrO_2$ mixed oxide (1:1 mole ratio) support was prepared by a homogeneous coprecipitation method using urea as precipitation reagent [33]. In brief, an aqueous mixture solution containing the requisite quantities of $TiCl_4$ (Fluka, AR grade), $ZrOCl_2$ (Fluka, AR grade) and urea (Loba Chemie, GR grade) were heated together to 368 K with vigorous stirring. The coprecipitate thus formed was filtered off, washed several times with deionized water until free from chloride ions and dried at 393 K for 12 h. The dried precipitate was finally calcined at 773 K for 6 h in open-air atmosphere. Some portions of this support was once again heated at 873, 973, and 1073 K for 6 h in a closed electrical furnace in open-air atmosphere.

A 12 wt.% $MoO_3/TiO_2–ZrO_2$ catalyst was prepared by a standard wet impregnation method. To impregnate MoO_3, the requisite quantity of ammonium heptamolybdate (J T Baker, England, AR grade) was dissolved in doubly distilled water and a few drops of dilute NH_4OH was added to make the solution clear and to keep the pH constant (pH 8).

Finely powdered calcined (773 K) mixed oxide support was added to this solution and the excess water was evaporated on a water bath with continuous stirring. The resultant solid was then dried at 383 K for 12 h and calcined at 773 K for 6 h in a closed electrical furnace in open-air atmosphere. Some portions of this finished catalyst was once again heated at 873, 973, and 1073 K for 6 h in a closed electrical furnace in open-air atmosphere.

2.2. Catalyst characterization

X-ray powder diffraction patterns have been recorded on a Siemens D-5000 diffractometer by using Cu Kα radiation source and Scintillation Counter detector. The XRD phases present in the samples were identified with the help of ASTM Powder Data Files. The X-ray line broadening technique was used to determine the crystallite size of $ZrMo_2O_8$ in the samples from XRD data of (1 1 2) reflection [34]. The FTIR spectra were recorded on a Nicolet 740 FTIR spectrometer at ambient conditions, using KBr discs, with a nominal resolution of 4 cm^{-1} and averaging 100 spectra.

The XPS measurements were made on a VG-ESCA lab 210 spectrometer (resolution 0.1 eV) with Mg Kα (1253.6 eV) radiation as the excitation source. The spectra were recorded in fixed analyzer transmission mode, the pass energy being 50 eV. The scanning of the spectra was done at pressures less than 10^{-8} Torr. Binding energies were measured for O (1s), Ti (2p), Mo (3d), and Zr (3d). The binding energy (BE) reference was taken at the Ti $2p_{3/2}$ of Ti^{4+} at 458.5 eV. An estimated error of $\pm$0.1 eV can be assumed for all the measurements. Quantification was accomplished by determining the elemental peak areas, following the Shirley background subtraction by the usual procedures [35,36]. Quantitative analysis of atomic ratios was carried out using the sensitivity factors supplied with the instrument. The modified Auger parameter of Ti was calculated according to the following equation:

$$\alpha^{I} = \alpha + h\nu = \text{BE of the Ti } 2_{3/2} \text{ peak} + \text{KE of the Ti } L_3M_{23}V \text{ Auger peak}$$

where BE is the binding energy and KE the kinetic energy.

3. Results and discussion

The TiO_2–ZrO_2 mixed oxide obtained by a homogeneous coprecipitation method and calcined at 773 K exhibited a BET surface area of 160 $m^2\,g^{-1}$. Therefore, a 12 wt.% of MoO_3 was used to impregnate on the titania–zirconia binary oxide support to achieve a monolayer coverage [37,38]. The XRD patterns of TiO_2–ZrO_2 calcined at various temperatures from 773 to 1073 K revealed that the mixed oxide support is in an X-ray amorphous or a poorly crystalline state up to 873 K calcination temperature [33]. However, the formation of crystalline $ZrTiO_4$ compound was clearly noted from 973 K and above temperatures in line with literature reports [28]. Further, the intensity of the lines due to $ZrTiO_4$ compound were also found to increase with increase in calcination temperature up to 1073 K. Most importantly, no independent lines due to TiO_2 (anatase or rutile) and ZrO_2 (monoclinic, tetragonal, or cubic) phases were observed even up to 1073 K. The observed higher stability of $ZrTiO_4$ compound up to 1073 K as well as its formation at lower temperatures was envisaged as due to a different preparation method adopted and the precursor compounds used for the preparation of this binary oxide support [33]. The XRD phases identified in the case of 12% MoO_3/TiO_2–ZrO_2 sample calcined at various temperatures are summarized in Table 1. These results

Table 1
Major XRD phases and IR bands present in 12 wt.% MoO_3/TiO_2–ZrO_2 catalyst calcined at different temperatures

Temperature (K)	XRD phases	$ZrMo_2O_8$ compound (crystallite size, nm)	IR bands (wave number, cm^{-1})
773	$ZrMo_2O_8$, $ZrTiO_4$	< 3.50	920, 980
873	$ZrMo_2O_8$, $ZrTiO_4$	< 3.50	920, 980
973	$ZrMo_2O_8$, $ZrTiO_4$, TiO_2 (rutile)	4.34	800, 920, 980
1073	$ZrMo_2O_8$, $ZrTiO_4$, TiO_2 (rutile)	4.44	800, 920, 980

show the formation of both $ZrTiO_4$ and $ZrMo_2O_8$ compounds with varying intensities depending on the calcination temperature. The $ZrTiO_4$ compound belongs to the space group *Pcnb* and has an orthorhombic structure of α-PbO_2 [39]. The transformation of amorphous TiO_2–ZrO_2 mixed oxide into a definite crystalline $ZrTiO_4$ compound at 873 K and above temperatures indicates that a high thermal energy is needed to promote interdiffusion of ions to form more ordered crystalline compound. The $ZrTiO_4$ compound is quite stable in the absence of MoO_3. This is evidenced by the absence of crystalline TiO_2 and ZrO_2 phases, even after high temperature treatments. It is well known in the literature that for molybdena contents of less than monolayer coverage the active component will be present as a two-dimensional molybdenum oxide overlayer on the support surface. Quantities in excess of monolayer coverage will have microcrystalline MoO_3 particles present on the catalyst surface in addition to the molybdenum oxide overlayer [12,40]. The observed $ZrMo_2O_8$ compound is expected to be formed at the expense of MoO_3 and amorphous or crystalline $ZrTiO_4$.

The XRD results reveal that the reactivity of molybdena towards $ZrTiO_4$ compound is very interesting. It appears from these results that molybdena reacts preferably with the ZrO_2 portion of $ZrTiO_4$ compound to form $ZrMo_2O_8$ phase, thus liberating the TiO_2. The size of Mo^{6+} resembles more with ZrO_2 making a uniform mixing of MoO_3 species with ZrO_2 support [41]. The portion of TiO_2 released from the $ZrTiO_4$ compound appears in the form of crystalline anatase or rutile phases as shown in Eq. (1):

$$ZrTiO_4 + 2MoO_3 \rightarrow ZrMo_2O_8 + TiO_2\,(\text{anatase and rutile}) \quad (1)$$

However, a different behavior was noted when V_2O_5/TiO_2–ZrO_2 catalyst was subjected to thermal treatments at different temperature [33]. The MoO_3 on TiO_2–ZrO_2 appears to behave differently and is less reactive towards the phase transformation of TiO_2 anatase-into-rutile when compared to V_2O_5 [42].

The FTIR spectrum of 12 wt.% MoO_3/TiO_2–ZrO_2 catalyst calcined at different temperatures from 773 to 1073 K has been recorded and the observed IR bands are presented in the Table 1. Generally, the IR band of Mo=O in crystalline MoO_3 appears at 1000 cm^{-1} due to stretching vibration mode. Frausen et al. [43] reported the formation of $ZrMo_2O_8$ compound by heating ZrO_2 and MoO_3 together at 820 K, which showed the IR bands at 980, 920 and 800 cm^{-1}. The FTIR results in the present study also revealed the formation of $ZrMo_2O_8$ compound and whose concentration was found to dependent on the calcination temperature employed. An interesting observation to be mentioned here is that irrespective of calcination temperature no characteristic bands due to crystalline MoO_3 are observed. In line with XRD observations, the formation of $ZrMo_2O_8$ compound was noted from FTIR study. The anatase and rutile phase of titania normally exhibits strong absorption bands in the region of 850–650 and 800–650 cm^{-1}, respectively. Presence of these phases, especially at 1073 K, was also noted from FTIR study in line with XRD observations.

X-ray photoelectron spectroscopy (XPS or ESCA), because of its high surface sensitivity (probing depth ca. 2 nm), has been considered as one of the best techniques for studying the dispersion of MoO_3 on various supports and to gain knowledge on the type of interaction involved between the active metal oxide species and the supporting oxide. In order to examine the nature of surface species formed at different temperatures the TiO_2–ZrO_2 support and the 12 wt.% MoO_3/TiO_2–ZrO_2 catalyst were investigated by XPS technique. The photoelectron peaks of O 1s, Ti 2p, Zr 3d, and Mo 3d are depicted in Figs. 1–4, respectively. For the purpose of better comparison, the XPS photoelectron peaks of O 1s, Ti 2p and Zr 3d pertaining to MoO_3/TiO_2–ZrO_2 catalyst and the corresponding peaks of TiO_2–ZrO_2 support are presented together in these figures. The Ti/Zr, Mo/Ti and Mo/Zr atomic percentage ratios as determined by XPS peak intensities are shown in Fig. 5 and Table 2. All these figures and table clearly indicate that the XPS bands depend on the calcination temperature and the coverage of molybdenum oxide on TiO_2–ZrO_2 mixed oxide carrier.

The O 1s profile, as presented in Fig. 1, is complicated due to the overlapping contribution of

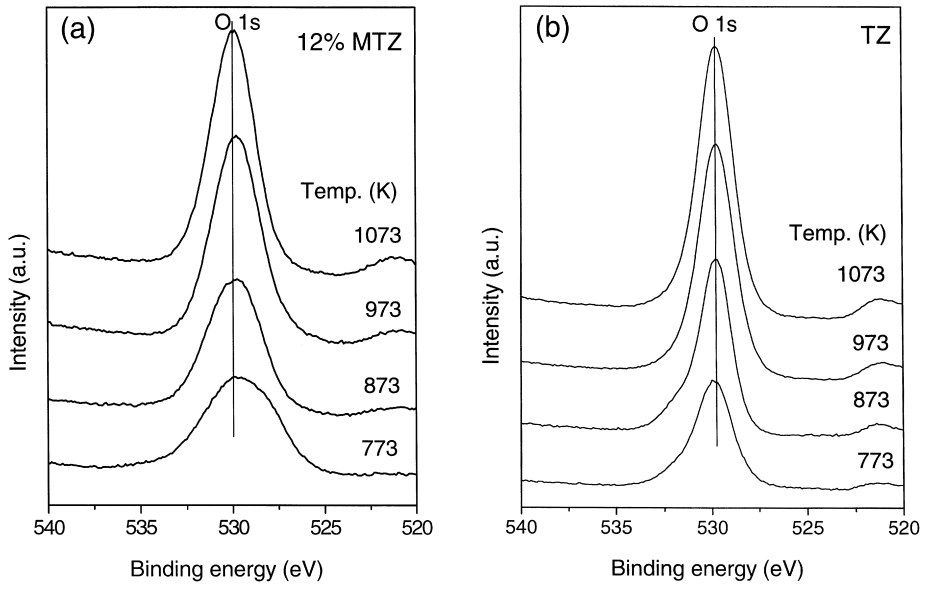

Fig. 1. XPS of the O 1s binding energy region for $MoO_3/TiO_2–ZrO_2$ catalyst and $TiO_2–ZrO_2$ support calcined at different temperatures.

oxygen from titania and zirconia in the case of $TiO_2–ZrO_2$ support, and to titania, zirconia, and molybdena in the case of the $MoO_3/TiO_2–ZrO_2$ catalyst, respectively. Fig. 2 shows the binding energies of Ti 2p photoelectron peaks at 458.5 and 464.4 eV for Ti $2p_{3/2}$ and Ti $2p_{1/2}$ lines, respec-

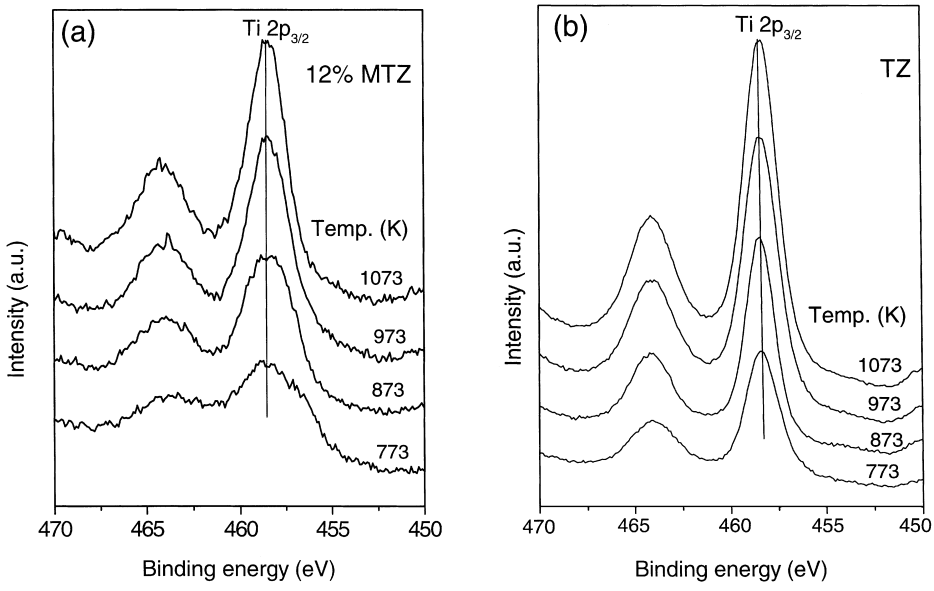

Fig. 2. Ti 2p XPS binding energy region for $MoO_3/TiO_2–ZrO_2$ catalyst and $TiO_2–ZrO_2$ support calcined at different temperatures.

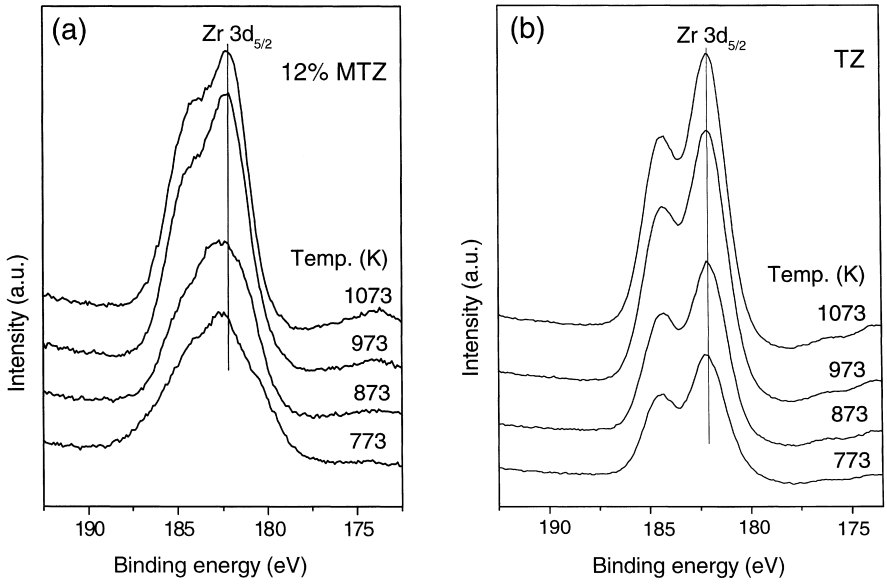

Fig. 3. Zr 3d XPS spectra of MoO_3/TiO_2–ZrO_2 catalyst and TiO_2–ZrO_2 support calcined at different temperatures.

tively, which agree well with the values reported in the literature [44,45]. As can be noted from Fig. 2 that there is an increase in the intensity of the Ti 2p photoelectron signals with increase in calcination temperature. The increase is more predominant for pure TiO_2–ZrO_2 than MoO_3/TiO_2–ZrO_2 catalyst, indicating that the intensity of Ti 2p photoelectron signals depend on the calcination temperature as well as on MoO_3 coverage on the TiO_2–ZrO_2 carrier. The Auger parameter for Ti has been measured and summarized in Table 2, showing very small and insignificant variation for both pure TiO_2–ZrO_2 support and MoO_3/TiO_2–ZrO_2 catalyst. As this parameter does not depend on charge effects, the Ti seems to be in a similar chemical state for all the samples. Therefore, Ti was considered as a good reference for binding energy calibrations. The measurement of the Auger parameter was envisaged by one of us recently as a good means of assessing the electronic properties of oxides dispersed on metal or metal oxide supports [46,47].

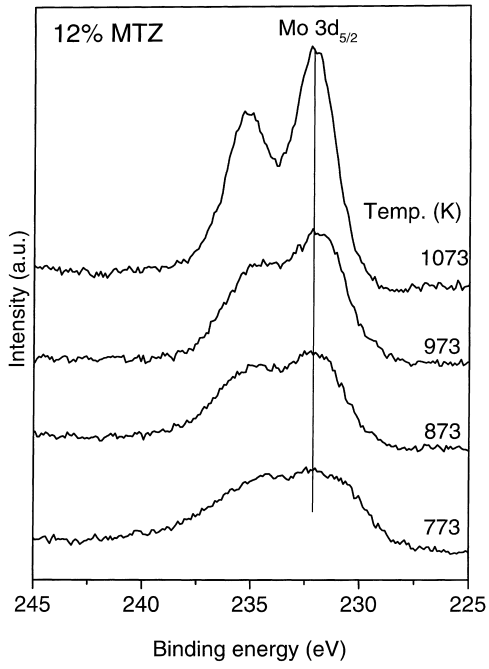

Fig. 4. Mo 3d XPS spectra of the MoO_3/TiO_2–ZrO_2 catalyst calcined at different temperatures.

The binding energy of the Zr 3d core levels are presented in Fig. 3 and Table 2 which show a slight decrease with increase in calcination temperature. This decrease in binding energy is more predominant in the case of MoO_3/TiO_2–ZrO_2 catalyst than that of pure support. This decrease in binding energy may presumably be due to the formation of new phases, i.e. $ZrTiO_4$, $ZrMo_2O_8$ compounds, respectively. An-

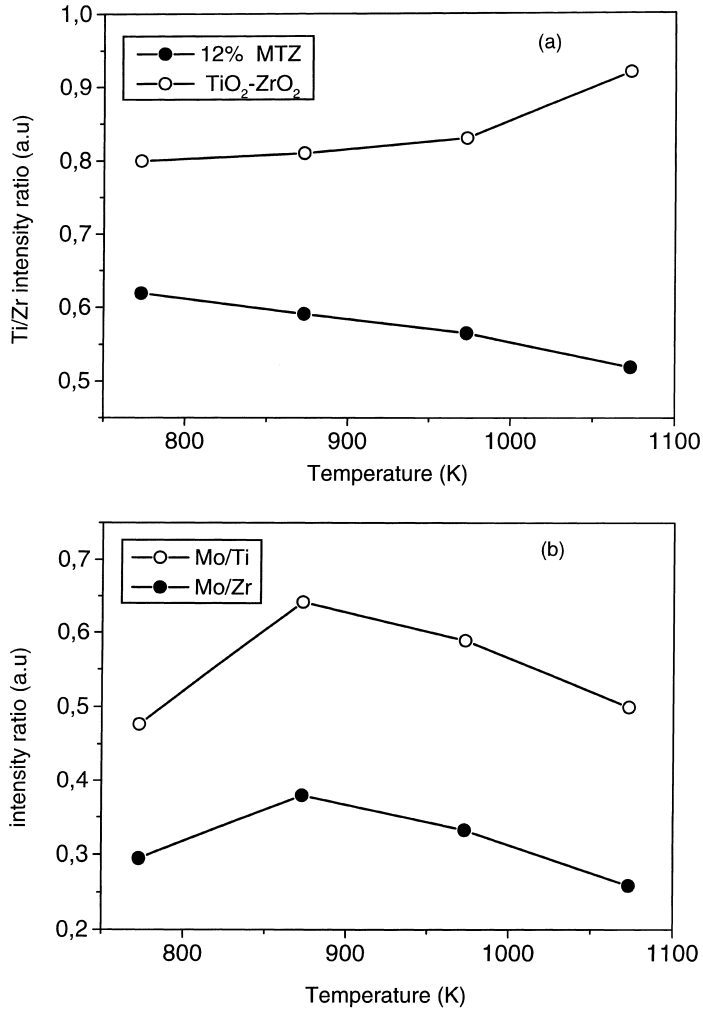

Fig. 5. XPS atomic ratio *versus* calcination temperature for the TiO_2–ZrO_2 support and MoO_3/TiO_2–ZrO_2 catalyst calcined at different temperatures.

other interesting observation to be mentioned here is that the Zr $3d_{5/2}$ core level peak was initially broad for MoO_3/TiO_2–ZrO_2 catalyst and both Zr $3d_{5/2}$ and Zr $3d_{3/2}$ peaks become prominent only at higher temperatures. However, the resolution of spin-orbit coupled peaks of Zr 3d core level was found to be better for the pure TiO_2–ZrO_2 support than MoO_3/TiO_2–ZrO_2 catalyst at all temperatures. The broadening of the Zr 3d peaks for the supported catalyst indicates an electronic interaction of ZrO_2 with MoO_3 in its dispersed state.

The Mo $3d_{5/2}$ photoelectron peak of MoO_3/TiO_2–ZrO_2 catalyst calcined at various temperatures is presented in Fig. 4. This figure clearly shows that there are significant differences in the local electronic environment of the surface molybdenum species at different temperatures. However, there is only a little variation in the core level binding energy (Table 2) while going from 773 to 1073 K temperature. The core level binding energy values indicate that molybdenum is present in Mo (VI) state in the catalyst. The Mo 3d photoelectron peak was very

Table 2
Binding energies, XPS atomic ratios, and modified auger parameter values for TiO_2–ZrO_2 support and 12 wt.% MoO_3/TiO_2–ZrO_2 catalyst calcined at different temperatures

Temperature (K)	O 1s	Ti		Zr $3d_{5/2}$	Mo $3d_{3/2}$	I_{Ti}/I_{Zr}	I_{Mo}/I_{Ti}	I_{Mo}/I_{Zr}
		$2p_{3/2}$	α^1 (Ti)					
TiO_2–ZrO_2 support								
773	530.0	458.5	873.6	182.5		0.80		
873	529.9	458.5	873.6	182.3		0.81		
973	529.8	458.5	873.6	182.3		0.83		
1073	529.7	458.5	873.6	182.3		0.92		
MoO_3/TiO_2–ZrO_2 catalyst								
773	529.9	458.5	873.3	182.7	232.1	0.62	0.48	0.29
873	529.7	458.5	873.5	182.5	231.8	0.59	0.64	0.38
973	529.5	458.5	873.6	182.3	231.7	0.56	0.59	0.33
1073	529.3	458.5	873.4	182.3	232.0	0.52	0.50	0.26

broad at lower temperatures and a better resolution of the spin-orbit coupled peak is noted at higher calcination temperatures. The broadening of the ESCA peak can be attributed to various factors including (i) the presence of more than one type of Mo (VI) with different chemical characteristics which cannot be discerned by ESCA [48], and (ii) electron transfer between active component and the support (metal-support interaction) [49]. The molecular structures of the surface molybdenum oxide species of the calcined samples generally dependent on the net surface pH at the point of zero charge (PZC). The PZC of a supported metal oxide catalyst depends on the nature of the support oxide involved. It has been proposed that the final pH of the solution in the filled pores of a support is close to the PZC of the support because of a fairly large buffer capacity of the support [50]. The amphoteric oxide supports, TiO_2 (anatase, pH at PZC ~ 6.2) and ZrO_2 (pH at PZC ~ 6.7), favor the formation of same octahedrally coordinated polymolybdate species at higher loadings [51]. Therefore, presence of chemically different molybdenum species can be avoidable in the case of lower temperature calcined samples. Thus, peak broadening can be attributed due to a charge transfer between the active component and the support oxide. It appears, however, that the charge transfer between molybdenum and the support is highly influenced by the local geometry and chemistry around the single Mo center. A better resolution of Mo $3d_{5/2}$ peak at higher temperatures is due to the formation of $ZrMo_2O_8$ compound where molybdenum has more uniform geometrical and chemical characteristics compared to the one present at lower calcination temperatures as a dispersed phase on the support surface. Thus, both different structure/chemistry and charge transfer lead to the signal broadening in the case of samples calcined at lower temperatures.

The dispersion of metals or metal oxides on various support surfaces can be estimated from ESCA intensity ratio measurements of different peaks [44,52,53]. Thus, obtained atomic ratios are presented in Fig. 5 and Table 2. As can be noted from Fig. 5, with increase in calcination temperature the Ti/Zr intensity ratio has been found to increase in the case of pure support and decrease for the molybdena doped samples. The decrease of Ti/Zr intensity ratio for molybdena impregnated samples may be due to the formation of $ZrMo_2O_8$ compound by interaction of molybdenum with zirconium thereby making the surface rich in zirconium. The numerical values of Ti/Zr intensity ratio for molybdena doped samples are found to be less than that of pure support. This may presumably be due to the surface coverage of molybdenum oxide on the mixed oxide support. The Mo/Ti and Mo/Zr intensity ratios are expected to provide information about the relative dispersion of molybdena component on the mixed oxide support. These ratios are found to increase

with increase in calcination temperature only up to 873 K. Sharp falls in the intensity ratios were found beyond this temperature. This variation in the intensity ratio is mainly due to a change in the surface distribution of molybdenum atoms on the surface of the support. Several models have been proposed in the literature to explain the dispersed state of molybdenum on different single oxide supports [1,11,12,13]. These models can be divided mainly into two categories: the first model suggests that under appropriate conditions a monolayer of the dispersed ionic compound is formed on the surface of the support, and the second model proposes that instead of forming an overlapping monolayer, the dispersed metal cations are incorporated into the surface vacant sites of the support with their accompanying anions staying on top of them for charge compensation. Livage et al. [54] have proposed that the amorphous zirconia consists of a layer of zirconium between two layers of oxygen with a structure similar to the (1 1 1) plane of tetragonal zirconia. It is known that tetragonal zirconia has slightly fluorite structure and only half of its distorted cube sites surrounded by oxygen anions are occupied by Zr^{4+} ions. With the assumption that (1 1 1) planes are preferentially exposed on the surface of the zirconia [55,56], its surface vacant sites can be used for the incorporation of the dispersed cations according to the incorporation model [57]. For $MoO_3/TiO_2–ZrO_2$ samples as the calcination temperature (773 K) is apparently higher than the Tamann temperature of MoO_3 (543 K) [1,58], it seems reasonable to consider that the probability of the dismantlement of the MoO_3 bulk phase into ion pairs or molecules at the temperature of calcination. The highly mobile Mo^{6+} ions that are formed might migrate and incorporate into the vacant sites available on the underlying surface of the ZrO_2 enhancing dispersion of Mo^{6+} ions on the surface [59]. In fact, the formation of $ZrMo_2O_8$ compound starts at 773 K temperature, as observed from XRD study, indicates incorporation of Mo^{6+} ions into the ZrO_2 support. This structural reorganization of the Mo-oxide on the support surface has been reflected on the initial increase of Mo/Ti and Mo/Zr intensity ratios. However, the newly formed $ZrMo_2O_8$ acts as a nucleation center for crystal growth at higher temperatures as can be noted from XRD study (Table 1). The crystallization reduces the dispersion of the molybdenum ion on the surface thereby lowering the Mo/Ti and Mo/Zr atomic ratios at temperatures beyond 873 K.

4. Conclusions

The following conclusions can be drawn from this investigation: (1) the $TiO_2–ZrO_2$ mixed oxide support when calcined at 773 K is in X-ray amorphous state and exhibits a high specific surface area. The amorphous $TiO_2–ZrO_2$ gets converted into $ZrTiO_4$ compound beyond 873 K calcination temperature and this compound is thermally quite stable even up to 1073 K in the absence of molybdena. It indicates that a high temperature is needed to promote interdiffusion of ions to form more ordered crystalline compound from the amorphous phase. (2) MoO_3 selectively interacts with ZrO_2 portion of $TiO_2–ZrO_2$ mixed oxide and readily forms $ZrMo_2O_8$ compound by liberating TiO_2. The liberated TiO_2 appears in the form of both anatase and rutile phases with varying intensities. The newly formed $ZrMo_2O_8$ compound is highly sensitive to the calcination temperature. The formation of this compound appears to proceed in a two step process. First there is an incorporation of Mo^{6+} ions into the ZrO_2 oxide matrix and is followed by its crystal growth. (3) At lower calcination temperatures molybdena interacts strongly with the mixed oxide support and will be present mostly in a dispersed state as observed from maximum broadening of the Mo 3d peak in the photoelectron spectra. Better resolution of Mo 3d at higher temperatures indicates that molybdenum has more uniform geometrical and chemical characteristics due to $ZrMo_2O_8$ compound formation. (4) The MoO_3 on $TiO_2–ZrO_2$ mixed oxide appears to be less reactive towards the phase transformation of TiO_2 anatase-into-rutile when compared to V_2O_5 on $TiO_2–ZrO_2$ [33].

The most interesting theory of promoter action in heterogeneous catalytic reaction is the role of interface between two surfaces of different compositions. There is abundant evidence in the literature that such linear interfaces often possess unusual reactive powers. The newly formed $ZrMo_2O_8$ compound might have created a new interface between the active

component and the support oxide phase, which was not present originally in the simple monolayer molybdena catalysts. Therefore, further study has been undertaken to investigate the influence of temperature on the reactivity of this interesting catalyst system.

Acknowledgements

EPR thanks the Dirección General de Investigación Científica y Técnica (Spain) for financial support. BC is the recipient of senior research fellowship of the University Grants Commission, New Delhi.

References

[1] H. Knözinger, E. Taglauer, Catalysis, The Royal Society of Chemistry, Vol. 10, Cambridge, 1993, p. 1 and references therein.
[2] A.N. Startsev, Catal. Rev.-Sci. Eng. 37 (1995) 353 and references therein.
[3] K. Segawa, I.E. Wachs, in: I.E. Wachs (Ed.), Characterization of Catalytic Materials, Butterworths–Heinemann, Boston, 1992, p. 72.
[4] J.R. Bartlett, R.P. Cooney, in: R.J.H. Clark, R.E. Hester (Eds.), Spectroscopy of Inorganic-Based Materials, Wiley, New York, 1987, p. 187.
[5] G. Mestl, T.K.K. Srinivasan, Catal. Rev.-Sci. Eng. 40 (1998) 451 and references therein.
[6] D.M. Hercules, J.C. Klein, in: H. Windawi, F.F.L. Ho (Eds.), Applied Electron Spectroscopy for Chemical Analysis, Wiley, New York, 1982.
[7] R. Prins, V.H.J. de Beer, G.A. Somorjai, Catal. Rev.-Sci. Eng. 31 (1989) 1.
[8] H. Topsøe, in: J.P. Bonnelle, B. Delmon, E. Derouane (Eds.), Surface Properties and Catalysis by Non-Metals, Reidel, 1983, p. 329.
[9] C. Martin, I. Martin, V. Rives, P. Malet, J. Catal. 147 (1994) 465.
[10] S. Rajagopal, H.J. Marini, J.A. Marzari, R. Miranda, J. Catal. 147 (1994) 417.
[11] H. Knözinger, in: M.J. Phillips, M. Ternan (Eds.), Proceedings of the Ninth International Congress of Catalysts, Vol. 5, Calgary, 1988. The Chemical Society of Canada, Ottawa, 1989, p. 20.
[12] F.E. Massoth, Adv. Catal. 27 (1978) 265 and references therein.
[13] W.K. Hall, in: H.F. Barry, P.C.H. Mitchell (Eds.), Proceedings of the Fourth Climax International Conference on Chemical and Uses of Molybdenum, Climax Molybdenum Co., Ann Arbor, MI, 1982, p. 224.
[14] C.C. Williama, J.G. Ekdert, J.M. Jehng, F.D. Hardcastle, I.E. Wachs, J. Phys. Chem. 95 (1991) 8791 and references therein.
[15] D. Vanhove, S.R. Op, A. Fernández, M. Blanchard, J. Catal. 57 (1979) 253.
[16] S. Okazaki, M. Kumasaka, J. Yoshida, K. Kosaka, K. Tanabe, Ind. Eng Chem. Prod. Res. Div. 20 (1981) 301.
[17] K. Tanaka, K.I. Tanaka, J. Chem. Soc. Chem. Commun. (1984) 748.
[18] K. Segawa, T. Soeya, D.S. Kim, Res. Chem. Intermed. 15 (1991) 129.
[19] J.G. Eon, E. Bordes, A. Vejux, P. Courtine, in: K. Dyrek, J. Haber, J. Nowtony (Eds.), Proceedings of the Ninth Symposium on the Reactivity of Solids, PWN, Warnzac, 1982, p. 603.
[20] P.D.L. Merceda, J.G. Van Ommen, E.B.M. Doesburg, A.J. Burggraaf, J.R.H. Ross, Appl. Catal. 57 (1990) 127 and references therein.
[21] B.M. Reddy, K.V.R. Chary, B.R. Rao, V.S. Subrahmanyam, C.S. Sunandana, N.K. Nag, Polyhedron 5 (1986) 191.
[22] D. Hamon, M. Vrinat, M. Breysse, B. Duyand, M. Jebrouni, M. Roubin, P. Magnoux, T.D. Courieres, Catal. Today 10 (1991) 613.
[23] Y. Matsuoka, M. Niwa, Y. Murakami, J. Phys. Chem. 94 (1990) 1477.
[24] T. Ono, H. Miyata, Y. Kubokawa, J. Chem. Soc., Faraday Trans. 83 (1987) 1761.
[25] B. Manohar, V.R. Reddy, B.M. Reddy, Synth. Commun. 28 (1998) 3183.
[26] W.M. Mullins, B. Averbach, Surf. Sci. 206 (1988) 29.
[27] J.C. Wu, S.C. Chung, A.Y. Ching-Lan, I. Wang, J. Catal. 87 (1984) 98.
[28] J. Fung, L. Wang, J. Catal. 130 (1991) 577.
[29] US Patent 5,576,467 (1996).
[30] I. Wang, W.H. Huang, C. Wu, Appl. Catal. 18 (1985) 273.
[31] K.Y.S. Ng, E. Gulari, J. Catal. 92 (1985) 340.
[32] C.V. Caceres, J.L.G. Fierro, J. Lazaro, A.L. Agudo, J. Soria, J. Catal. 122 (1990) 113.
[33] B.M. Reddy, B. Manohar, S. Mehdi, J. Solid State Chem. 97 (1992) 233.
[34] H.P. Klug, L.E. Alexander, X-ray Diffraction Procedures for Polycrystalline and Amorphous Materials, 2nd Edition, Wiley, New York, 1974.
[35] A. Savitzky, M.J.E. Golay, Anal. Chem. 36 (1964) 1627.
[36] D.A. Shirley, Phys. Rev. B 5 (1972) 4709.
[37] A.J. Van Hengstun, J.G. Van Ommen, H. Bosch, P.J. Gellings, Appl. Catal. 5 (1983) 207.
[38] D.S. Kim, Y. Kurusu, I.E. Wachs, F.D. Hardcastle, K. Segawa, J. Catal. 120 (1989) 325.
[39] Y. Park, Mater. Res. Bull. 33 (1998) 1325.
[40] B.M. Reddy, K.S.P. Rao, V.M. Mastikhin, J. Catal. 113 (1988) 556.
[41] T. Ono, H. Kamisuki, H. Hisashi, H. Miyata, J. Catal. 116 (1989) 303.
[42] B.M. Reddy, E.P. Reddy, S. Mehdi, Mater. Chem. Phys. 36 (1994) 276.

[43] T. Frausen, P.C. Van Berge, P. Mars, Preparation of Catalysts I, Elsevier, Amsterdam, 1976, p. 405.
[44] B.M. Reddy, B. Chowdhury, I. Ganesh, E.P. Reddy, T.C. Rojas, A. Fernández, J. Phys. Chem. B 102 (1998) 10176.
[45] G.A. Sawatzky, D. Post, Phys. Rev. B20 (1979) 1546.
[46] J.A. Mejías, V.M. Jiménez, G. Lassaletta, A. Fernández, J.P. Espinós, A.R. González-Elipe, J. Phys. Chem. 100 (1996) 16255.
[47] A. Fernández, A. Caballero, A.R. González-Elipe, Surf. Interface Anal. 18 (1992) 392.
[48] P. Ratnasamy, J. Catal. 40 (1975) 137.
[49] N.K. Nag, J. Phys. Chem. 91 (1987) 2324.
[50] L. Wang, W.K. Hall, J. Catal. 66 (1980) 251.
[51] G. Deo, I.E. Wachs, J. Phys. Chem. 95 (1991) 5889.
[52] D. Briggs, J. Electron Spectrosc. Relat. Phenom. 9 (1976) 487.
[53] Y. Okamoto, H. Tomioka, Y. Katoh, T. Imanaka, S. Teranishi, J. Phys. Chem. 84 (1980) 1833.
[54] J. Livage, K. Doi, Mazieres, J. Am. Ceram. Soc. 51 (1968) 349.
[55] J.R. Anderson, Structure of Metallic Catalysts, Academic Press, New York, 1975, p. 62.
[56] C. Morterra, G. Cerrato, L. Ferroni, L. Montaro, Mater. Chem. Phys. 37 (1994) 247.
[57] Y. Chen, L. Dong, Y.S. Jin, B. Xu, W.J. Ji, Stud. Surf. Sci. Catal. 101 (1996) 1293.
[58] Y. Chen, L.F. Zheng, Catal. Lett. 12 (1992) 51.
[59] Z. Liu, Y. Chen, J. Catal. 177 (1998) 314.